

Extracting Broken-Rotor-Bar Fault Signature of Varying-Speed Induction Motors

Dehong Liu, Anantaram Varatharajan, and Abraham Goldsmith

Mitsubishi Electric Research Laboratories, Cambridge, MA, 02139, USA

{liudh,varatharajan,goldsmith}@merl.com

ABSTRACT

An effective way to detect broken-bar faults of squirrel-cage induction motors is to extract the characteristic frequency component in the stator current as a fault signature, or so-called motor current signature analysis (MCSA). However, for inverter-fed motor drive systems, the motor is typically operating under varying-speed, varying-load, and noisy environments, which makes the fault signature extraction a very challenging problem. In this paper, we propose a sparsity-driven and graph-based method to extract the fault signature effectively, where the fault signature is modeled as a sparse component in the frequency domain for each short-time window measurement while gradually changing from window to window in the time-domain. Compared to the conventional short-time Fourier transform-based method, our method is more robust to noise and varying speed operations. Experiments are carried out to demonstrate the effectiveness of the proposed method.

1. INTRODUCTION

Squirrel-cage induction motors are widely used in various kinds of fields such as water pump, power fan, and industrial drive, *etc.*, for their low price and high efficiency. However, squirrel-cage induction motors are typically operating in very severe environments and consequently subject to different types of faults. Besides insulation faults and electric faults (short circuit), mechanical faults such as bearing faults and broken-bar faults are also very common after years of operations due to wearing bearings and pulsating forces on rotor bars. Once a mechanical fault occurs, excessive vibration, poor starting performance, and torque fluctuation will be induced during operation, accelerating the system failure if the motor is not well maintained. Therefore, it is very important to monitor the motor health condition such that timely maintenance and predictive maintenance can be made for safe operations.

Dehong Liu et al. This is an open-access article distributed under the terms of the Creative Commons Attribution 3.0 United States License, which permits unrestricted use, distribution, and reproduction in any medium, provided the original author and source are credited.

For line-fed induction motors under steady operation conditions, it is straightforward to extract fault signatures. Although multiple symptoms can be utilized to detect motor faults, a widely used non-invasive method is to monitor the stator current and further to detect the fault signature via motor current signature analysis (MCSA). In general, when a motor fault occurs, the rotating magnetic field is no longer symmetric as desired. Consequently, rotating-speed-dependent frequency components are generated in the stator current. Therefore, these frequency components can be treated as fault signature for motor health monitoring, and different types of faults correspond to different characteristic frequency. Since the motor is operating at steady state, the frequency spectrum change be easily achieved by Fourier transform based methods.

While nowadays inverter-driven instead of line-fed induction motors are becoming more and more popular in industrial applications with the development of AC drive and control technologies for the sake of efficiency, it is challenging to extract the motor current fault signature due to the following reasons: 1) the amplitude of stator current varies due to load variation; 2) the rotating speed is also variable in a large range; and 3) the inverter may introduce extra interference to the current measurement. In this situation, conventional Fourier transform-based methods are either no longer applicable or with poor performance in motor fault detection and health monitoring.

Researchers have been developing rotor fault detection methods for motors operating at non-stationary conditions for decades, mainly based on short-time Fourier transform (STFT). For example, in (Fernandez-Cavero, Morinigo-Sotelo, Duque-Perez, & Pons-Llinares, 2017), an adaptive transform utilizes a function called the time-frequency atom that allows for precise observation of fault components in transient regimes. These methods allow tracking the fault-related frequency by performing relevant time-frequency (t-f) transform. The drawback is that the energy of the fault-related frequency component is much lower than the fundamental one, which makes it difficult to differentiate due

to spectral leakage (Garcia-Calva, Morinigo-Sotelo, Garcia-Perez, Camarena-Martinez, & de Jesus Romero-Troncoso, 2019). In recent years, sparsity-driven methods have been applied in fault signature extraction (Liu & Lu, 2015; Kelkar, Liu, Inoue, & Kanemaru, 2023) to achieve improved detection performance. These methods make use of sparsity to either achieve a super spectral resolution (Liu & Lu, 2015) or compensate the influence of the varying load (Kelkar et al., 2023). However, all these sparsity-driven methods assume the fault frequency is time-invariant, which may be not true for practical inverter-drive motor systems.

In this paper, we study the broken-bar fault signature under varying speed conditions. In order to effectively extract broken-bar fault signature of induction motors under varying operation conditions, we model the stator current as a graph with nodes represented by sliding small time windows of the stator current. A weighted adjacency matrix represents the pairwise proximity between nodes (time windows) is then estimated and utilized for further analysis. Following the idea of graph model, we propose a graph-based method to extract the fault signature by solving an optimization problem with constraints imposing sparsity and smoothness of the fault signature in the stator current spectrogram. Compared to the conventional short-time Fourier transform-based method, our method is more robust to noise and varying speed operations. Experiments are carried out to demonstrate the effectiveness of the proposed method.

2. GRAPH-BASED FAULT SIGNATURE EXTRACTION

2.1. Fault Signature

For a healthy induction machine, its stator current contains a fundamental frequency component and harmonics of the fundamental frequency in inverter-fed applications. When a rotor bar is broken, additional frequency components f_b are induced in the stator current

$$f_b = (1 \pm 2\kappa s)f_s, \quad (1)$$

where f_s is the fundamental supply frequency; s is the slip; and $\kappa = 1, 2, \dots$. MSCA-based broken-bar fault detection techniques focus on detecting the dominant frequency component or so-called characteristic frequency component in the stator current, which is

$$f_{b1} = (1 - 2s)f_s. \quad (2)$$

We ignore the detailed physical model of electric machines, which can be found in many literatures such as (Krause, Wasynczuk, Sudhoff, & Pekarek, 2013), and focus on the signal processing part of the fault detection. The three-phase stator current for a faulty induction machine can be simplified

as

$$i_a(t) = I_1 \cos(\omega_s t) + I_{brb} \cos(\omega_{brb} t + \phi_{brb}), \quad (3)$$

$$i_b(t) = I_1 \cos(\omega_s t - 2\pi/3) + I_{brb} \cos(\omega_{brb} t + \phi_{brb} - 2\pi/3), \quad (4)$$

$$i_c(t) = I_1 \cos(\omega_s t + 2\pi/3) + I_{brb} \cos(\omega_{brb} t + \phi_{brb} + 2\pi/3), \quad (5)$$

where I_1 and I_{brb} represents the amplitude of the fundamental component and the fault component, respectively; ω_s and $\omega_{brb} = (1 - 2s)\omega_s$ is the angular frequency of the power supply and of the fault component, respectively; and ϕ_{brb} is the phase angle of the fault component. In inverter-fed drive applications where the motor operation speed is variable, both ω_s and ω_{brb} may be changing along with time.

2.2. Graph Model of Fault Signature

A commonly used approach to processing a non-stationary signal is to represent it in the time-frequency domain using the short-time Fourier transform (STFT). In particular, the non-stationary signal is partitioned into short-time pieces using overlapped sliding-time windows. Each windowed piece of signal is analyzed using the fast Fourier transform (FFT), providing frequency spectrum information within the local time duration.

By performing STFT on the stator current of a single phase or a combination of three-phase current, a matrix of signal spectrogram is obtained as $\mathbf{Y} = [\mathbf{Y}_1, \dots, \mathbf{Y}_m, \dots, \mathbf{Y}_M]$, in which the column vector \mathbf{Y}_m represents the frequency spectrum of the m^{th} windowed signal of the stator current. Each row of \mathbf{Y} corresponds to a fixed frequency value. To avoid redundancy, we only consider frequency range $[0, F_s/2]$, where F_s is the frequency sampling rate of stator current measurements. Since both the operating speed and the load are changing, the fault signature frequency is not a constant, meaning that the fault signature component in the spectrogram matrix does not lie in any single row vector of a certain frequency, but a slowly changing curve related to the motor speed.

Motivated by recent progress in graph signal processing, we treat the current spectrogram as a graph signal observed from graph $G = (\mathbf{V}, \mathbf{A})$, where $\mathbf{V} = \{v_1, \dots, v_m, \dots, v_M\}$ is the set of nodes, represented by sequential moving time windows, and $\mathbf{A} \in R^{M \times M}$ is the graph shift, or a weighted adjacency matrix that represents the pairwise proximity between nodes. Associated with the m^{th} node (time window) of the graph, a N -dimensional frequency spectrum vector $\mathbf{Y}_m \in C^N$ is achieved by analyzing the time-domain measurements $\mathbf{y}_m \in R^{2N}$ via Fourier transform (FT) or other methods such as minimum-variance (MV)-based spectral analysis (Liu, Inoue, & Kanemaru, 2022) for better denoising performance. We can estimate the graph shift \mathbf{A} through the STFT frequency

spectra as

$$A_{i,j} = \frac{|\mathbf{Y}_i^H \mathbf{Y}_j|}{\sqrt{\mathbf{Y}_i^H \mathbf{Y}_i} \sqrt{\mathbf{Y}_j^H \mathbf{Y}_j}}, \text{ for } |i - j| < d, \quad (6)$$

where the superscript H indicates the matrix Hermitian transpose, d is the maximal distance of connected neighborhood nodes in the graph. When stator current measurements are taken in overlapped time windows, the measurements should have strong pairwise correlations in the frequency domain.

Therefore, the spectrogram matrix of the stator current at varying speed and varying load can then be treated as a noisy graph signal with an unknown frequency shift due to the varying operation, *i.e.*,

$$\mathbf{Y}_m = \mathbf{X}_m + \mathbf{N}_m, \text{ for } m = 1, \dots, M, \quad (7)$$

where $\mathbf{X} = [\mathbf{X}_1, \dots, \mathbf{X}_m, \dots, \mathbf{X}_M]$ represents the denoised spectrogram and \mathbf{N}_m is signal noise.

2.3. Graph-based Fault Signature Extraction

Inspired by recent research work on graph-model based signal denoising (Chen, Sandryhaila, Moura, & Kovacevic, 2014; Liu, Chen, & Boufounos, 2020), we extract the fault signature by solving an optimization problem as

$$\min_{\mathbf{X}} \sum_{m=1}^M \frac{1}{2} \|\mathbf{X}_m - \mathbf{Y}_m\|_2^2 + \lambda R_1(\mathbf{X}) + \beta R_2(\mathbf{X}), \quad (8)$$

where λ and β are hyper-parameters, $R_1(\mathbf{X})$ and $R_2(\mathbf{X})$ are regularizing terms. $R_1(\mathbf{X})$ imposes sparsity of the graph signal using L_1 norm as

$$R_1(\mathbf{X}) = \|\mathbf{X}\|_1 = \sum_{m=1}^M |\mathbf{X}_m|_1. \quad (9)$$

$R_2(\mathbf{X})$ promotes smoothness of graph signals, *i.e.*, neighboring nodes should share a similar fault signature in the frequency domain. $R_2(\mathbf{X})$ can be expressed as

$$R_2(\mathbf{X}) = \frac{1}{2} \|\mathbf{X} - \bar{\mathbf{A}}\mathbf{X}\|_F^2, \quad (10)$$

where $\bar{\mathbf{A}}$ is a normalized graph shift matrix whose entries are computed as $\bar{A}_{i,j} = \frac{A_{i,j}}{\sum_j A_{i,j}}$ to ensure that the sum of each row of $\bar{\mathbf{A}}$ equals to 1; the subscript F denotes the Frobenius norm.

The goal is to recover a clean spectrogram \mathbf{X} which possibly includes the fault signature from the noisy spectrogram \mathbf{Y} . The intuition behind the proposed graph-based denoising approach can be explained in two aspects: 1) the characteristic frequency component (or the fault signature) and the operating frequency component in each time window are sparse

(non-zero) components while other frequency components will be zeros, resulting a sparse frequency spectrum and 2) the rotor fault frequency component and the operating frequency component in consecutive time windows are smoothly changing and have strong pairwise correlation. Once we obtain continuously changing sparse frequency components forming a curve in the spectrogram besides the operating frequency components, we declare that we successfully extract the fault signature.

To solve the optimization problem, we adopt the augmented Lagrangian scheme, and apply the alternating direction method of multipliers (ADMM) to solve it (Wang, Yin, & Zeng, 2019). The whole fault signature extraction process can be summarized as in Algorithm 1, where \mathbf{I} is an identity matrix and $S_{\frac{\lambda}{\rho}}$ is a soft-thresholding function (Donoho, 1995) defined as

$$S_{\frac{\lambda}{\rho}}(z) = \max(|z| - \frac{\lambda}{\rho}, 0)z/|z|. \quad (11)$$

When the input z is a vector or a matrix, the soft-thresholding function works as an element-wise operator on each entry.

Algorithm 1 Graph-model-based fault signature extraction

- 1: **Input** : Time-domain stator current \mathbf{y} , parameters λ , β , and ρ .
- 2: Compute \mathbf{Y} using STFT or MV-based method.
- 3: Estimate \mathbf{A} and $\bar{\mathbf{A}}$.
- 4: Initialize $k = 1$, $\mathbf{Z}^{(0)} = 0$, and $\mathbf{W}^{(0)} = 0$.
- 5: **while** \mathbf{X}_k is not converged **do**

$$\begin{aligned} \mathbf{X}^{(k)} &\leftarrow [(\rho + 1)\mathbf{I} + \beta(\mathbf{I} - \bar{\mathbf{A}})^T(\mathbf{I} - \bar{\mathbf{A}})]^{-1} \\ &\quad [\mathbf{Y} + \rho(\mathbf{Z}^{(k-1)} - \mathbf{W}^{(k-1)})], \\ \mathbf{Z}^{(k)} &\leftarrow S_{\lambda/\rho}(\mathbf{X}^{(k)} + \mathbf{W}^{(k-1)}), \\ \mathbf{W}^{(k)} &\leftarrow \mathbf{W}^{(k-1)} + \mathbf{X}^{(k)} - \mathbf{Z}^{(k)}, \end{aligned}$$

- 6: **end while**
 - 7: **Output** : $\hat{\mathbf{X}} = \mathbf{X}^{(k)}$.
-

3. EXPERIMENTS

3.1. Set up

To validate our method, we perform experiments on a 1HP three-phase squirrel-cage induction motor. The experimental setup is shown in Fig. 1(a), where the motor is driven by a three-phase inverter. A servo-motor is mounted on the induction motor shaft and well aligned to work as a controllable load, whose speed and torque can be controlled precisely for the experiment purpose. The three-phase stator currents are measured using three current sensors and recorded using a computer interface for further analysis.

For comparison, we use two rotors of the same specifications, and manually produce a broken-bar fault on one of the two rotors by drilling a hole on a rotor bar. Pictures of the healthy

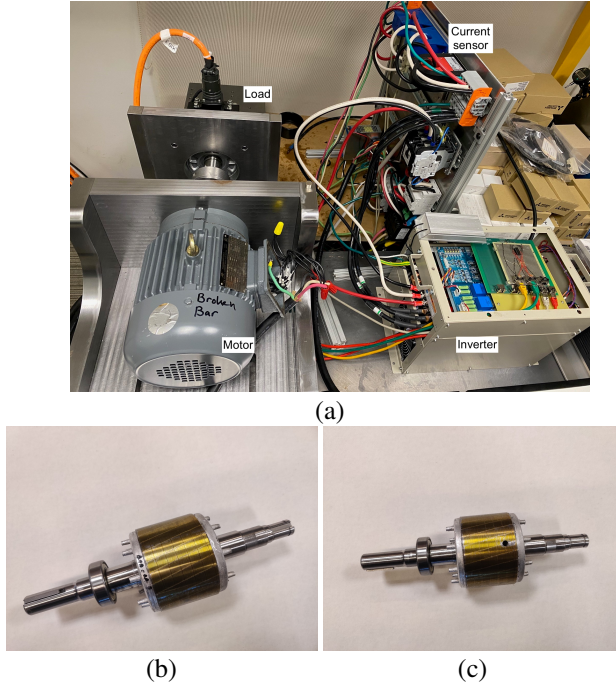


Figure 1. (a) Experimental setup, (b) Healthy rotor, and (c) Faulty rotor.

rotor and the faulty rotor are shown in Fig. 1 (b) and (c) respectively. Considering practical varying torque, varying-speed operations, we perform two experiments. In the first experiment we manually control the load torque (servo-motor), and in the second one we manually control the motor speed by varying the operating frequency, both following random and smooth speed patterns.

3.2. Varying load operation

An example of the time-domain stator current of the motor operating at varying load condition is shown in Fig. 2 (a), where we record about 53 second time-domain data with a sampling rate of 2kHz. We plot its Fourier spectrum of frequency from zero to 100Hz in Fig. 2 (b). It is clear that due to the varying load, the stator current amplitude changes from time to time. As a result, the characteristic frequency (fault signature) is not a constant frequency any more, but slowly changing from time to time.

To analyze the spectrogram with respect to time, we consider three different methods: (1) short-time Fourier transform (2) minimum variance-based spectral analysis, and (3) sparsity-driven graph-model-based method. For fair comparison, we use the same sliding time window of 2.5 seconds long, with 2 seconds overlap from window to window. For the graph-model-based method, we set parameters $\beta = 0.01$, $\rho = 0.02$, and $\lambda = 0.004 \times \max(|\mathbf{Y}_m|)$. The results are shown in Fig. 3 (a), (b), and (c), respectively. While the spectrogram is denoised using MV-based spectral analysis, it was cleaned

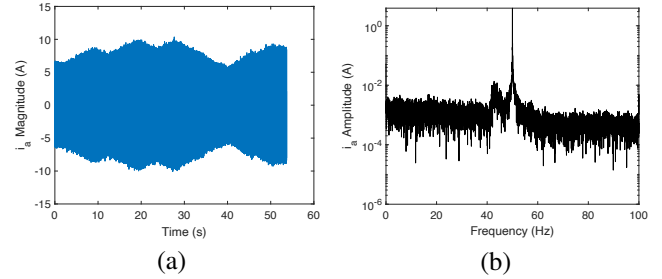


Figure 2. Stator current of varying load operation in (a) time-domain and (b) frequency-domain using Fourier transform.

further more by using the sparsity-driven graph-model-based method. We also show the ideal spectrogram according to Eq. (2) in Fig. 3 (d). We observe that the sparsity-driven graph-model-based result agrees with the ideal spectrogram very well.

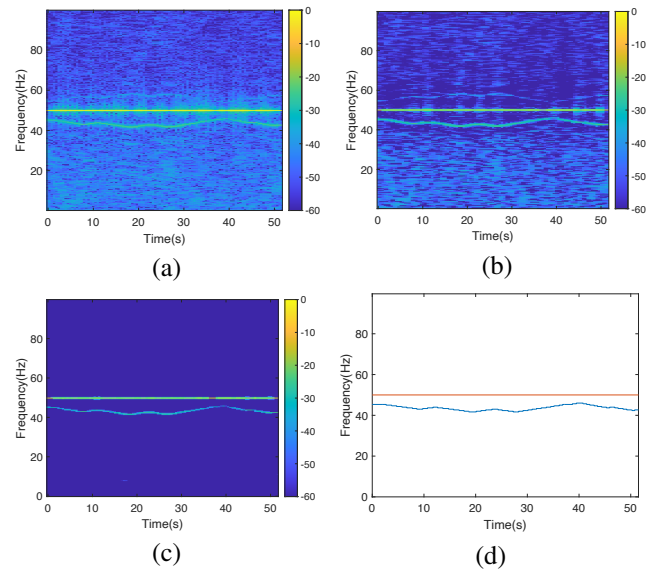


Figure 3. Spectrogram of stator current using (a) Short-time Fourier transform, (b) Minimum-variance based method, (c) Graph-based fault signature extraction, and (d) Ideal situation using Eq. (2).

3.3. Varying frequency operation

When the operating frequency is changed by the controller, the motor speed is also changing accordingly. An example of the time-domain stator current of the motor operating at varying frequency condition is shown in Fig. 4 (a) with the frequency spectrum using the Fourier transform in Fig. 4 (b). We observe that both the operating frequency and the characteristic fault frequency vary slowly from time to time.

Similarly, the spectrogram using three aforementioned methods are shown in Fig. 5 (a), (b), and (c), respectively. Again, our sparsity-driven graph-based method achieved the best

performance in extracting the fault signature. For comparison, we also show the spectrogram of a healthy motor operating at varying frequency conditions in Fig. 5 (d). It is clear that only the dominant operating frequency component can be detected.

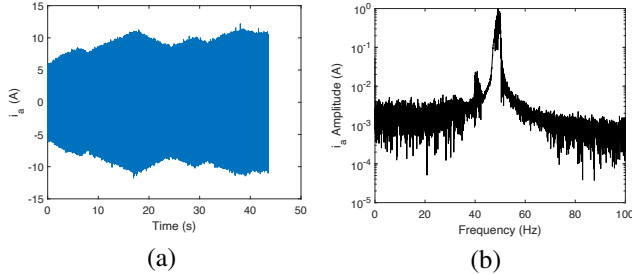


Figure 4. Stator current of varying frequency operation in (a) time-domain and (b) frequency-domain using Fourier transform.

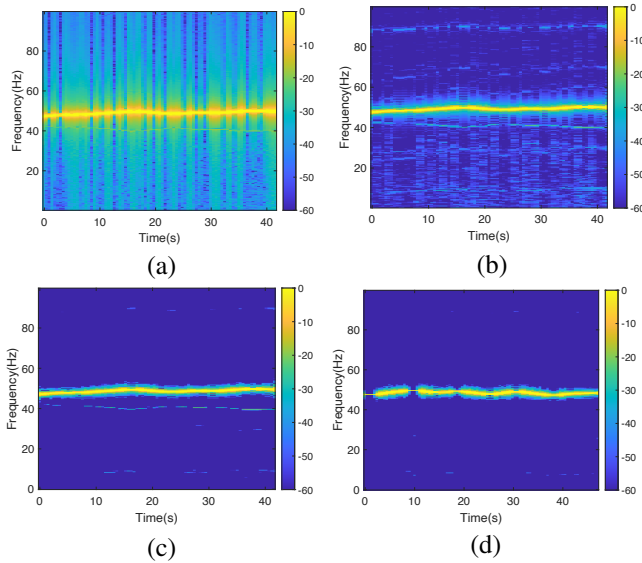


Figure 5. Spectrogram of stator current using (a) Short-time Fourier transform, (b) Minimum-variance based method, and (c) Graph model-based method, all for faulty motor except (d) Graph-model-based method for healthy motor.

4. CONCLUSION

We studied broken-rotor-bar fault detection for the inverter-fed squirrel-cage induction motor under varying speed and varying load conditions, and defined a fault signature using complex space vector notation. To extract the fault signature, we proposed a graph-based method by solving an optimization problem with constraints imposing smoothness and

sparsity of the fault signature. Experimental results demonstrate that our proposed method can effectively extract fault signature under varying speed and varying frequency operations. The newly revealed fault signature detection method is applicable for both line-fed and inverter-fed induction motor drives.

REFERENCES

- Chen, S., Sandryhaila, A., Moura, J. M., & Kovacevic, J. (2014). Signal denoising on graphs via graph filtering. In *2014 IEEE Global Conference on Signal and Information Processing (GlobalSIP)* (pp. 872–876).
- Donoho, D. L. (1995). De-noising by soft-thresholding. *IEEE transactions on information theory*, 41(3), 613–627.
- Fernandez-Cavero, V., Morinigo-Sotelo, D., Duque-Perez, O., & Pons-Llinares, J. (2017). A comparison of techniques for fault detection in inverter-fed induction motors in transient regime. *IEEE Access*, 5, 8048–8063.
- Garcia-Calva, T. A., Morinigo-Sotelo, D., Garcia-Perez, A., Camarena-Martinez, D., & de Jesus Romero-Troncoso, R. (2019). Demodulation technique for broken rotor bar detection in inverter-fed induction motor under non-stationary conditions. *IEEE Transactions on Energy Conversion*, 34(3), 1496–1503.
- Kelkar, V. A., Liu, D., Inoue, H., & Kanemaru, M. (2023). Sparsity-driven joint blind deconvolution-demodulation with application to motor fault detection. In *Icassp 2023-2023 IEEE International Conference on Acoustics, Speech and Signal Processing (ICASSP)*.
- Krause, P. C., Wasynczuk, O., Sudhoff, S. D., & Pekarek, S. D. (2013). *Analysis of electric machinery and drive systems* (Vol. 75). John Wiley & Sons.
- Liu, D., Chen, S., & Boufounos, P. T. (2020). Graph-based array signal denoising for perturbed synthetic aperture radar. In *Igarss 2020-2020 IEEE International Geoscience and Remote Sensing Symposium* (pp. 1881–1884).
- Liu, D., Inoue, H., & Kanemaru, M. (2022). Robust motor current signature analysis (mcsa)-based fault detection under varying operating conditions. In *2022 25th International Conference on Electrical Machines and Systems (ICEMS)* (pp. 1–5).
- Liu, D., & Lu, D. (2015). Off-the-grid compressive sensing for broken-rotor-bar fault detection in squirrel-cage induction motors. *IFAC-PapersOnLine*, 48(21), 1451–1456.
- Wang, Y., Yin, W., & Zeng, J. (2019). Global convergence of admm in nonconvex nonsmooth optimization. *Journal of Scientific Computing*, 78, 29–63.